Autonomous Remote Crack Displacement Monitoring of a Residence Near a Limestone Quarry, Naples, Florida

David E. Kosnik

ABSTRACT: This report describes the technology and methods deployed in the continuous autonomous remote monitoring of cracks in interior and exterior walls of a residence near a limestone quarry. The object is to quantitatively compare crack response to blast-induced ground motion to that induced by diurnal or daily temperature changes, weather fronts, and occupant activity. The remote monitoring system described has operated continuously and autonomously since June 2007. Data are made available for review in near-real time via a password-protected web site. Complementary web sites display measurements made for research and compliance purposes

INTRODUCTION

New communication technology may provide the means to mitigate the effect of public concerns about potential impacts of ground vibrations inherent in construction and production of raw materials. These concerns result in delays and increased costs for construction and raw materials. For instance, neighbors of road aggregate quarries often perceive that their houses are being damaged by vibration resulting from blasting at the quarry. Subsequent litigation and community action often increases the cost of aggregate, which increases the construction cost of any new projects in the area served by that quarry.

This new communication technology consists of four components: displacement sensors with micro-inch resolution, autonomous computer control, robust high-speed communication, and Internet display of results. New sensors capable of measuring micro-meter displacements can be employed to compare the long-term (climatological) and dynamic (ground motion and occupant activity) response of cracks. Comparison of the response of the same crack to both long-term and dynamic phenomena can be employed to distinguish large "silent" effects of weather from smaller but noisy effects of ground motion. Data from these sensors are electronically recorded and communicated back to a central digital repository. The data are then autonomously displayed via the Internet for public inspection. It is hoped that such unmoderated, on-demand public interaction with the measurements will allow greater involvement with the vibration monitoring program.

Definition of Crack Displacement

Advanced sensor and data acquisition technology make it possible to address concerns of vibration-induced cracking by directly measuring crack response. All

residences contain cracks to some extent, whether initiated by climatological effects, differential settlement, or other environmental factors. As such, cracks for measurement are readily available. A particular advantage of direct measurement of cracks is that the long-term and dynamic response may be simultaneously measured for the same crack. Crack response is measured in terms of *crack displacement*, i.e., change in crack width, rather than total crack width, as shown in Figure 1. Since it is a measure of change rather than absolute crack width, crack response may be positive (crack opening) or negative (crack closing).

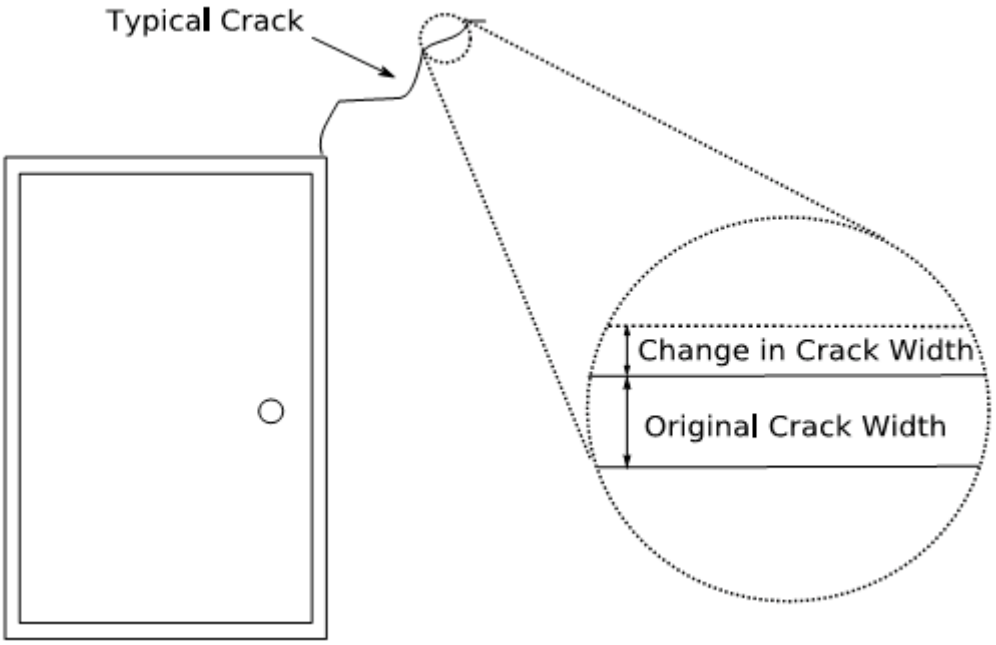

Figure 1: Definition of crack displacement, after Siebert (2000)

Residential Test Structure

The test structure's proximity to the blasts involved in this report is shown in Figure 3. The base map was copied from a USGS topography map. Complementary ground motion measurements for some events were also made at a site on 56th Ave NE, near the eastern property line of the quarry, which is also shown in Figure 3. Seismographs are shown by stars and blasts by dots. The test structure is a slab-on-grade house with CMU exterior walls. An elevation view of the house is shown in Figure 2.

Figure 2: West side of instrumented house

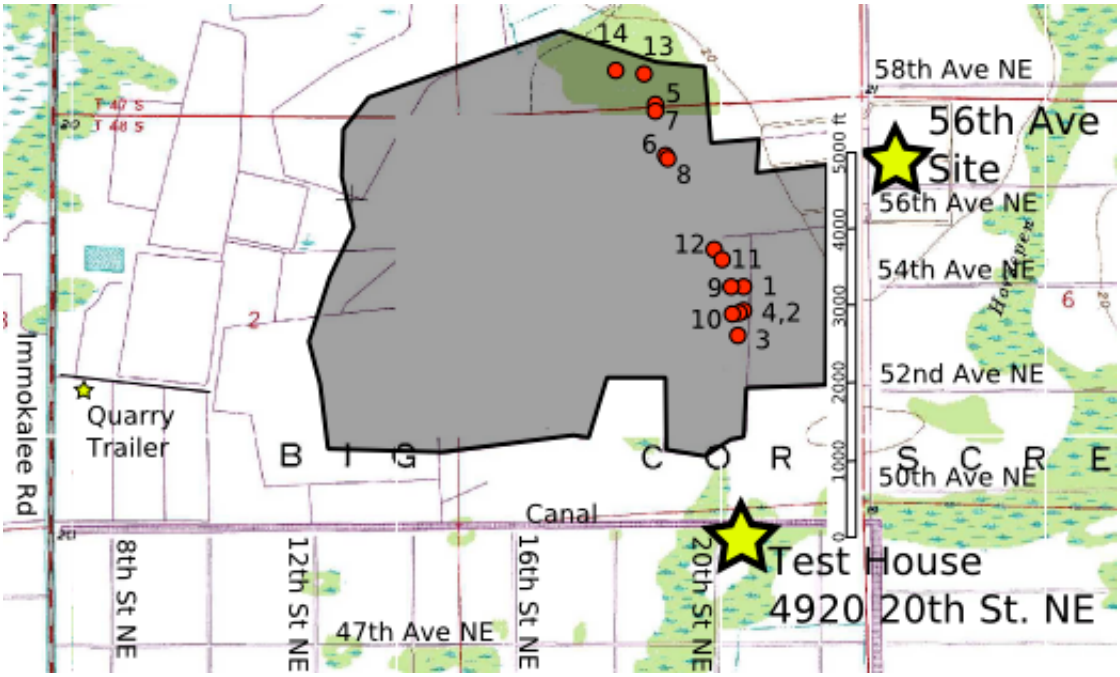

Figure 3: Topographic map of quarry, with instrumented test house (4920 20th St NE) and additional geophone site on 56th Ave NE (stars), blast locations (dots) and scale (in feet) superimposed

INSTRUMENTATION PLAN

Two complementary instrumentation systems are employed in the house: a research-oriented system from Northwestern University, and a commercial system from GeoSonics, Inc. Both systems measure crack displacement and ground motion; however, since the GeoSonics system is used for compliance, only the GeoSonics ground motion waveforms are considered for analysis. The Northwestern ground motion transducer was used only to trigger recording of dynamic events. Locations of all sensors from both systems are shown in Figure 4. Three cracks were selected for monitoring with the Northwestern system: two in south-facing exterior walls and one in an interior wall. At each crack, one displacement transducer was installed across the crack while an identical "null" transducer was positioned on a nearby area of un-cracked wall surface. Indoor and outdoor temperature and humidity sensors were installed to measure daily and long-term environmental changes. Two cracks were selected for monitoring with the GeoSonics system: one each on the interior and exterior of the west wall of the garage. As with the Northwestern system, both active and null transducers were installed at each crack.

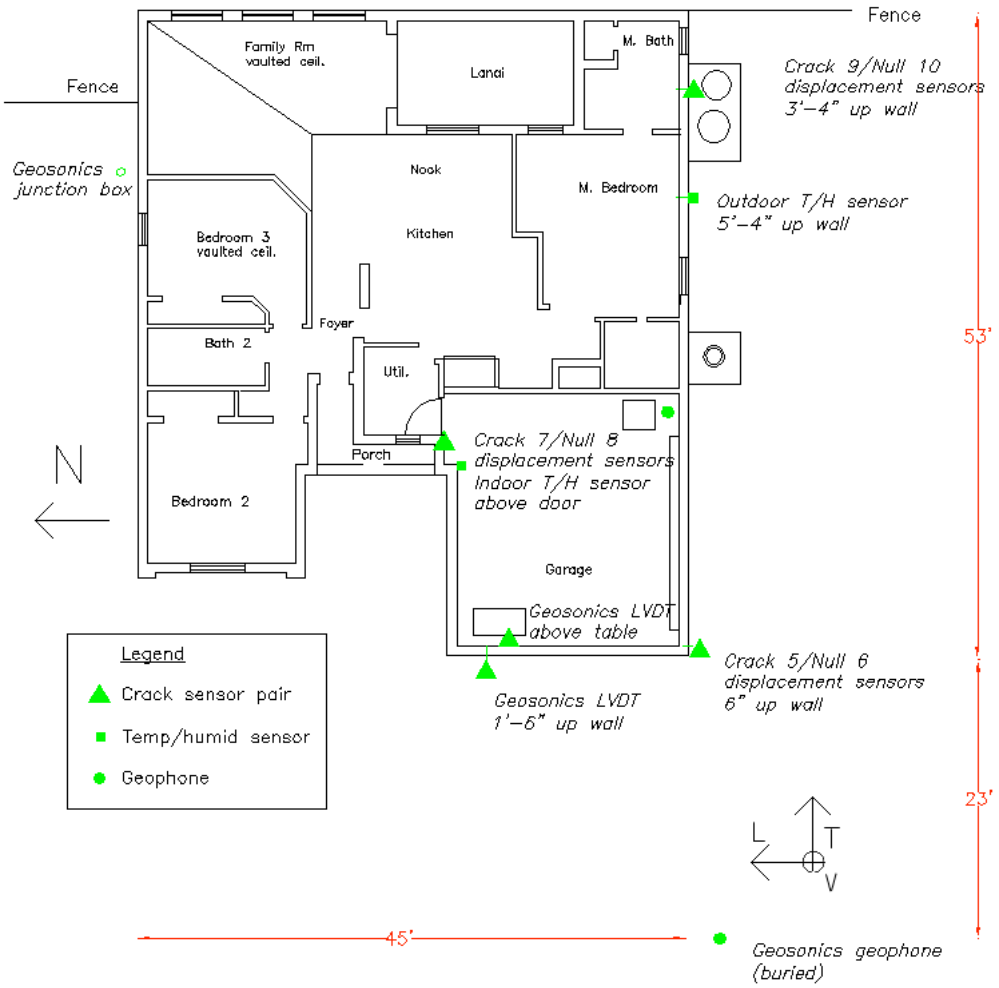

Figure 4: Instrumentation plan

Crack Displacement Transducers

A variety of microinch-resolution linear displacement transducers are commercially available. These devices are typically designed for use industrial control systems; as such, they are built for harsh environments and are generally well-suited for field applications. Kaman SMU-9000 non-contact eddy current displacement transducers were employed in the Northwestern University instrumentation. Suitability of these transducers for crack displacement monitoring was described by Siebert (2000) and Louis (2000). These transducers do not require physical contact across the crack and are thus less subject to binding or stick-slip behavior should large crack displacement occur in a direction normal to that measured by the instrument. Another advantage of the eddy-current sensors is the reduced footprint on the wall. Sensor and target brackets, which are firmly coupled to the wall with epoxy, are small, involving a total area of less than one square inch of wall surface. The electronics box that accompanies the sensor may be secured to the wall through less permanent means, such as double-stick tape. Consequently, eddy-current sensors are ideal for residences and other situations where the need for post-project repairs must be minimized. For instance, eddy-current gauges have been successfully deployed and removed even in an historic building subject to Federal preservation regulations (Baillot, 2004). The GeoSonics system uses free-core LVDT displacement sensors. Both Siebert and Louis showed that these devices are also suitable for long-term and dynamic microinch-range measurement of cracks, although they require attachment across the crack and have a larger footprint on the wall.

The three cracks instrumented by Northwestern represent a variety of cracking situations. The cracks are identified by their data acquisition channel numbers. Crack 5 is on the exterior stucco-over-CMU wall at the southwest corner of the house, approximately six inches from the ground. Crack 7 is on a gypsum-board wall inside the garage, above the door into the utility room. Crack 9 is located on the south exterior stucco wall, three feet above the ground. The three cracks are subject to different levels of solar radiation. Inside the garage, Crack 7 is never exposed to direct sunlight. On the south-facing exterior wall, Crack 5 is partially shaded by a shrub, while Crack 9 is in direct sunlight for much of the day. The trend of each crack is generally vertical. Close-up photographs of each crack are shown in the insets in Figure 5.

Ground Motion

Two geophones are employed; one for the GeoSonics instrumentation and one for the Northwestern instrumentation. Both are triaxial geophones manufactured by GeoSonics, Inc. The GeoSonics geophone is buried approximately 23 feet west of the southwest corner of the house with the longitudinal axis oriented north-south, along the general direction to the blasting areas in the quarry. For the GeoSonics instrumentation, the geophone serves both to trigger recording of dynamic events and measure ground particle velocity. The Northwestern geophone is coupled with epoxy directly to the slab in the southeast corner of the garage. The Northwestern geophone

serves only to trigger recording of dynamic events, since it is located within the structure. Excitation history should be measured outside the structure to avoid contamination with equipment or structural response.

(a) South face of house **(b)** Crack 5

(c) Crack 7 **(d)** Crack 9

Figure 5: General locations of crack displacement transducers, with insets showing detail of cracks and sensors

Temperature and Relative Humidity

Sensitivity of cosmetic cracks in residential structures to climatological has been described in previous work such as Dowding and McKenna (2005). Thus, it is necessary to monitor local climatological conditions at this test structure. To describe the temperature and humidity environment inside the garage, a Vaisala HMW-50 temperature/humidity transducer was installed on the north wall of the garage near Crack 7. A Vaisala HMT-100 temperature/humidity transducer was installed on the exterior wall of the house near Crack 9. The outdoor sensor is exposed to direct sunlight for much of the day, as is Crack 9. GeoSonics records local weather conditions with instruments mounted on a pole in the yard northwest of the house.

DATA ACQUISITION

Computer-controlled data acquisition is central to both the Northwestern and GeoSonics instrumentation systems. In both cases, the data acquisition system handles analog-to-digital conversion, dynamic triggering, and data logging. The Northwestern system is based on a Somat Corporation *eDaq* data acquisition technology. Two types of data are acquired: hourly "long-term" measurements and triggered dynamic events. Long-term data are recorded hourly from all displacement transducers as well as indoor and outdoor temperature and humidity sensors. These data are used to quantify the cracks' response to daily, frontal, seasonal, and other weather changes. Time histories of ground particle velocity and crack response to blasts and other transient events are recorded via dynamic triggering. Dynamic recording is triggered when one or more geophone channels exceed a threshold ground particle velocity. Once the system is triggered, crack displacement and triaxial ground particle velocity are recorded at 1000 samples per second. Since these events may occur at random, a 1000 ms pre-trigger buffer of data is stored by the data acquisition system at all times. The complete waveform recorded by the data acquisition system is four seconds long: one second of pre-trigger data followed by three seconds of post-trigger ground motion and crack response.

CRACK RESPONSE TO DYNAMIC EVENTS

Cracks in structures respond to a variety of dynamic events. While the response to blast-induced ground motion is of primary interest, diverse phenomena as operation of heavy construction equipment (Snider, 2003; Baillot, 2004), wind gusts (Dowding and Aimone-Martin, 2007), truck traffic, thunder, and everyday household activities (Louis, 2000) have been observed to have dynamic crack displacement effects. The dynamic effects of blast vibration and household occupant activities are presented in this report.

Ground motion is measured on three axes: longitudinal (L), transverse (T), and vertical (V). The orientation of the axes is labeled in Figure 4. Table 1 compares the PPV in these three directions with the maximum zero-to-peak crack displacement measured during each event. As will be shown later, ground motions (blast vibrations) with larger peak particle velocities produce greater crack responses.

Eighteen blasts were conducted at the quarry between June 20 and December 13, 2007 (Jones, 2007). Peak particle velocity recorded on the longitudinal, transverse, and vertical geophone axes as well as the maximum zero-to-peak crack displacement on each of the three cracks during the event are shown in Table 1. Also shown in Table 1 are the available shot details such as distance to the geophone (in

cases where motion was recorded at the structure) and charge weights per delay. The event on December 13 at 2:01 pm was a test shot conducted for demonstration purposes. It used a charge weight per hole half that of the regular production shot which followed at 2:19 pm. Figure 6 compares the time histories of ground motion and crack response for the August 21 event, which included the largest dynamic crack response observed in the study (456μin on Crack 7). Figure 7 presents response spectra for ground motion in the transverse direction for the August 21 event as well as the August 15 event. The spectra show that there are two principal frequencies of excitation: one at 8 Hz and another in the 10-15 Hz range.

Table 1: Summary of blast event parameters, including peak ground particle velocity (PPV), maximum dynamic crack response, distance *R* to instrumented house, explosive charge weight *W* per hole, and total number of holes loaded with explosive charges.

Shot	Date and Time		Geophone PPV (in/sec)			Crack Response (μin)			R (ft)	W (lbs)	No. of holes
			L	T	V	5	7	9			
1	2007-06-20	10:49:52	0.040	0.055	0.060	82	388	81	3258	78	78
2	2007-06-22	10:56:42	0.050	0.045	0.065	70	300	66	2930	71	78
3	2007-06-29	10:44:35	0.070	0.080	0.073	132	417	98	2623	155	76
4	2007-07-03	10:43:24	0.075	0.103	0.093	167	447	111	2910	155	69
5	2007-07-09	10:47:28	0.033	0.028	0.033	No data			5731	70	101
6	2007-07-17	10:52:23	0.033	0.038	0.030	No data			5041	70	96
7	2007-07-19	10:49:21	0.033	0.035	0.028	58	170	46	5619	70	99
8	2007-07-24	10:24:46	No data			58	194	49	5016	70	99
9	2007-08-09	10:12:44	0.067	0.098	0.077	134	330	70	3273	139	69
10	2007-08-15	11:10:20	0.100	0.092	0.103	207	407	123	2859	129	69
11	2007-08-21	10:26:37	0.095	0.087	0.073	200	456	112	3621	135	94
12	2007-08-27	11:07:20	No data			No data			3735	99	89
13	2007-09-07	9:49:55	0.032	0.037	0.039	122	158	46	6137	75	78
14	2007-09-13	10:46:23	0.015	0.020	0.023	No data			6266	60	43
15	2007-09-19	10:27:55	0.025	0.020	0.025	No data			-	51	-
16	2007-11-30	10:31:55	No data			No data			-	30	-
17	2007-12-13	13:59:04	0.045	0.040	0.048	144	317	90	-	25	-
18	2007-12-13	14:17:53	0.043	0.065	0.065	170	385	85	-	50	-

For the events for which location data were available, blasting was conducted between 0.5 to 1.2 miles from the instrumented structure, and charge weights between 25 and 155 pounds of explosives were loaded in each borehole (Jones, 2007). Ground motion at the instrumented structure is a function of the amount of explosives detonated at any particular instant (i.e., amount in a single hole without decks), rather than the total amount detonated in the course of the blast (Dowding, 1996).

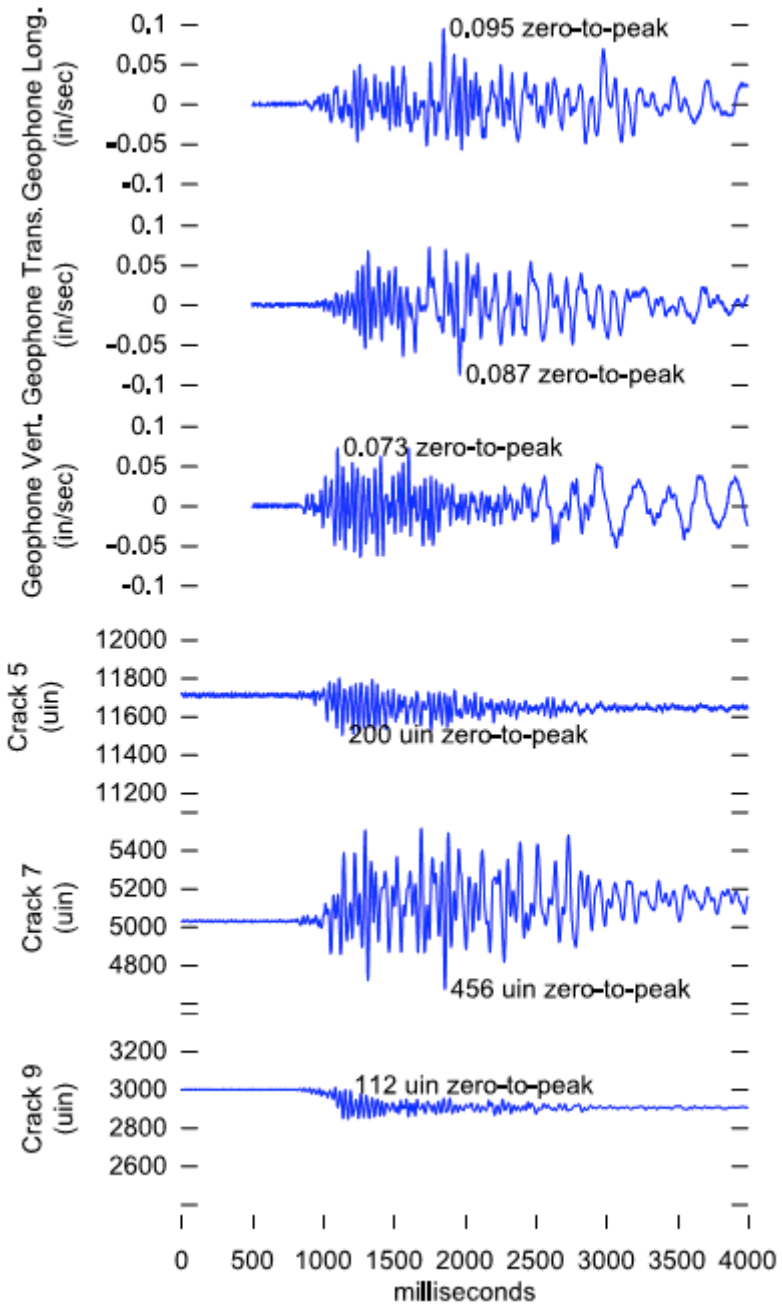

Figure 6: Comparison of triaxial ground motion and crack response time histories from the August 21 event

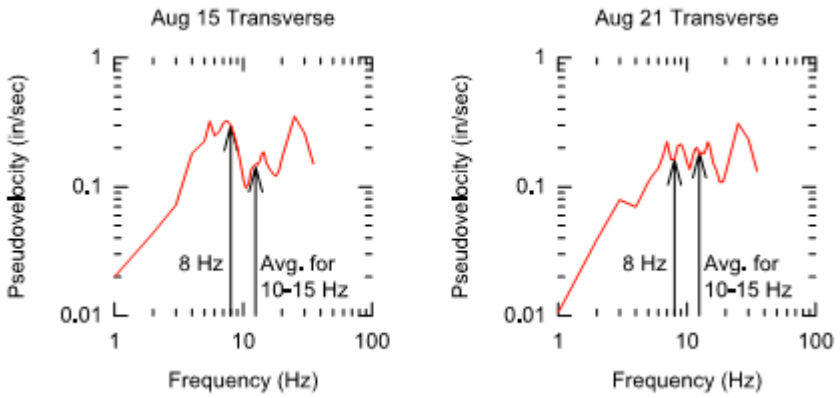

Figure 7: SDOF pseudovelocity response spectrum of transverse ground motion from August 15 and August 21 events, showing difference in response at estimated natural frequencies of superstructure (8 Hz) and walls (10-15 Hz)

Ground motion decays rapidly with distance, as shown in Figure 8, a plot of peak particle velocity (PPV) versus distance from the blast to the test house. Particle velocity is the speed with which a particle in the ground moves up and down as the ground motion passes by. The largest magnitude zero-to-peak ground particle velocities recorded by the GeoSonics geophone during the course of the study on the longitudinal, transverse, and vertical axes were, respectively, 0.100, 0.103, and 0.103 inches per second.

Figure 9 displays the same data as in Figure 8, except distance is given as the square-root scaled distance

$$SD = \frac{R}{\sqrt{W}} \qquad (1)$$

where R is the distance in feet and W is the explosive charge weight in pounds per delay. Either Figure 8 or 9 may be employed to estimate peak particle velocity at the structure of concern.

Figures 10 and 11 show attenuation of ground motion with distance by comparing the peak ground particle velocities induced at both the test house and a complementary geophone site on 56th Ave NE. The location of the additional site relative to the test house is shown in Figure 3. Measurement of motion induced by the same blast at multiple locations eliminates variations in blast design from the attenuation analysis. Figure 11 presents the same data as Figure 10, except distance is given as the square-root scaled distance, as described above.

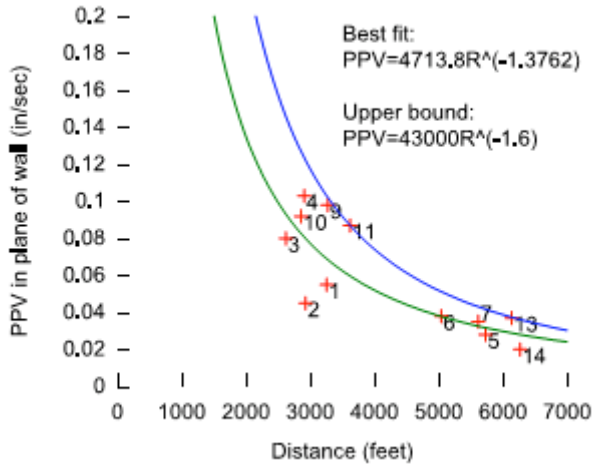

Figure 8: Attenuation of peak particle velocity with distance from blast site to test house. Numbers correspond to blasts listed in Table 1.

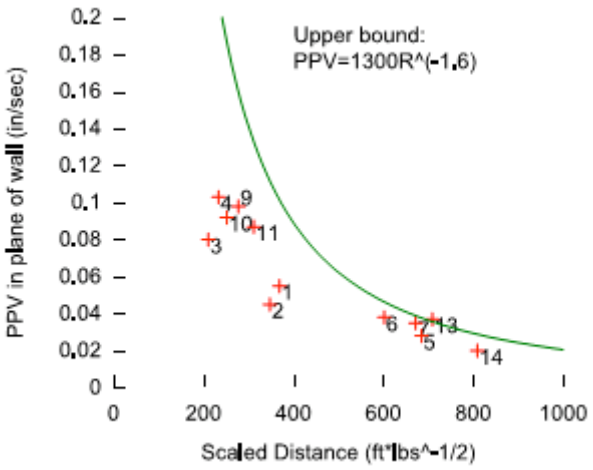

Figure 9: Attenuation of peak particle velocity with scaled distance from blast site to test house. Numbers correspond to blasts listed in Table 1.

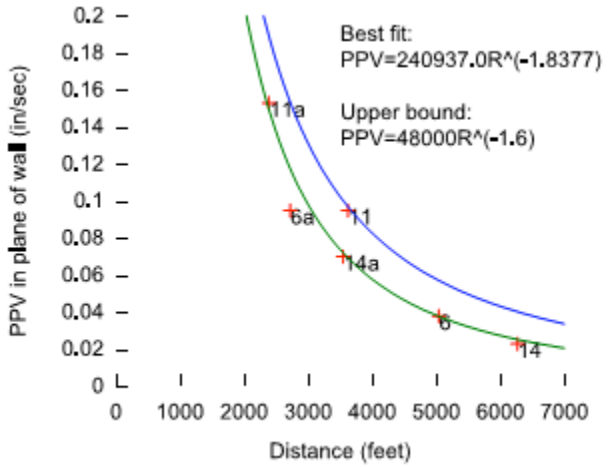

Figure 10: Attenuation of peak particle velocity with distance for three blasts for which data from multiple geophones were available. Numbers correspond to blasts listed in Table 1. Numbers alone represent data from the test house; numbers followed by *a* represent data from the complementary geophone site on 56th Ave NE.

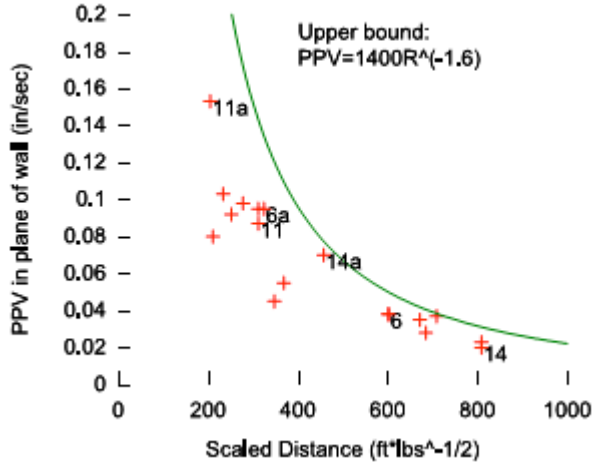

Figure 11: Attenuation of peak particle velocity with distance for three blasts for which data from multiple geophones were available. Numbers correspond to blasts listed in Table 1. Numbers alone represent data from the test house; numbers followed by *a* represent data from the complementary geophone site on 56th Ave NE.

Crack Response to Ground Motion

Sensitivity of a crack to ground motion may be compared to a variety of descriptors of either ground or structure motion. Sensitivity will be defined as the measured zero-to-peak dynamic response of the crack. Ground motion descriptors include peak particle velocity on each of the three orthogonal axes, the instantaneous vector sum of ground particle velocity along the three axes, and integration of the ground particle velocity waveform with respect to time to obtain displacement. Structural motion descriptors include the single degree of freedom (SDOF) model of structure response at its estimated natural frequency of 8 Hz, or the average response between 10 and 15 Hz, to capture possible wall response.

Sensitivity of crack response to various measures of excitation are shown in Figures 12, 13, and 14 for Cracks 5, 7, and 9, respectively. Crack responses are correlated with ground motion measures in the top row of the figure. All of these motions for comparison with crack response are in the transverse direction, which is parallel to the walls that contain the cracks. This parallel motion has been shown to be important in describing in-place shear distortion of the wall and the cracks (Dowding, 1996). Crack responses to SDOF estimates of structural motion at frequencies of 8 Hz and 10-15 Hz are shown in the bottom row of each figure.

The SDOF model estimates structure response through analysis of the full waveform of the excitation. Thus it includes measures of both peak motion as well as the frequency of excitation. By selecting structure response frequencies that model the superstructure (8 Hz) or the walls (10-15 Hz), it may be possible to discern which crack responses are due to superstructure or wall motions. In these comparisons, the damping coefficient was taken as 5% for all frequencies. The response spectrum shown in Figure 7 shows the different excitation response at the respective natural frequencies of the superstructure and the walls.

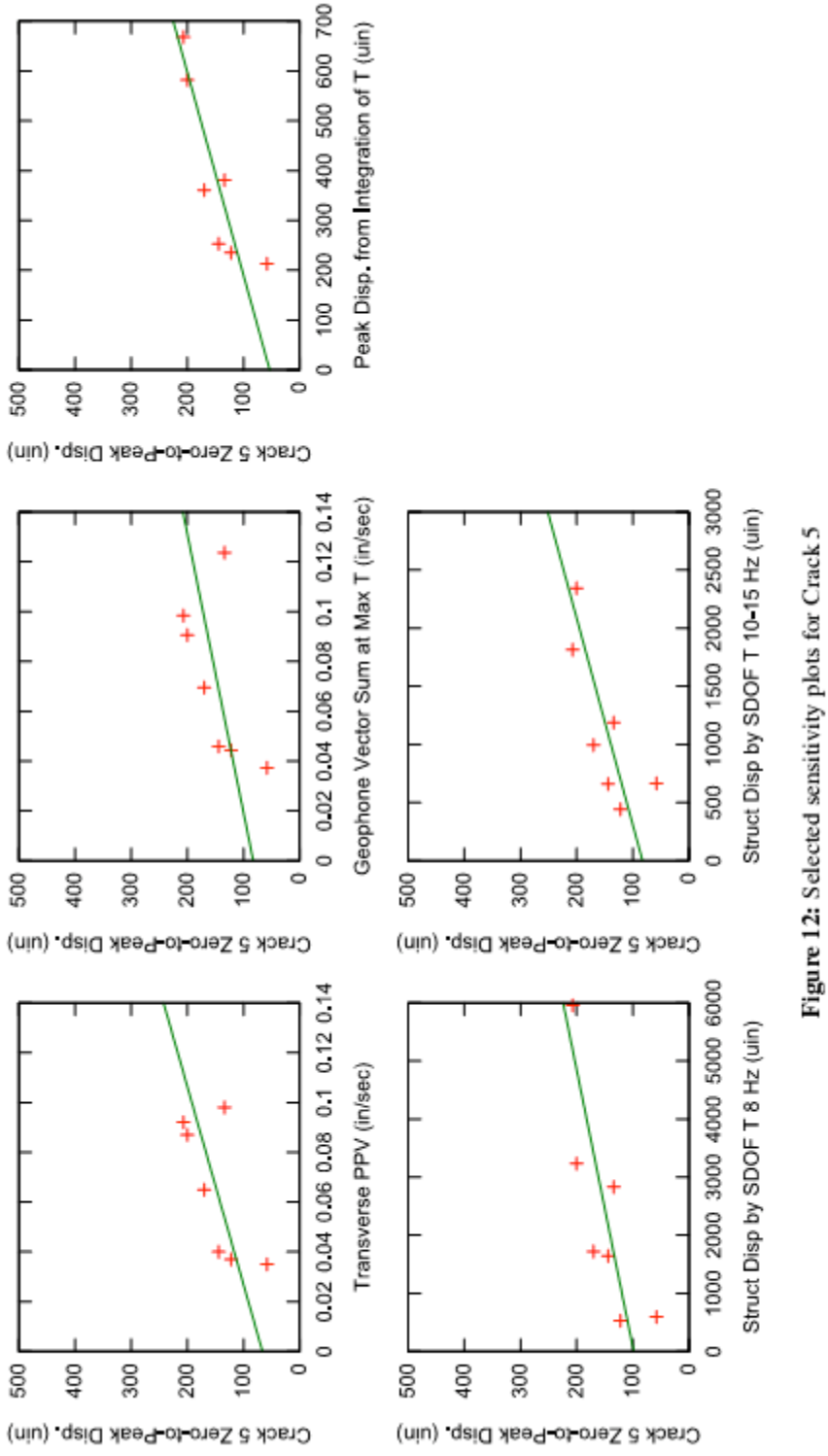

Figure 12: Selected sensitivity plots for Crack 5

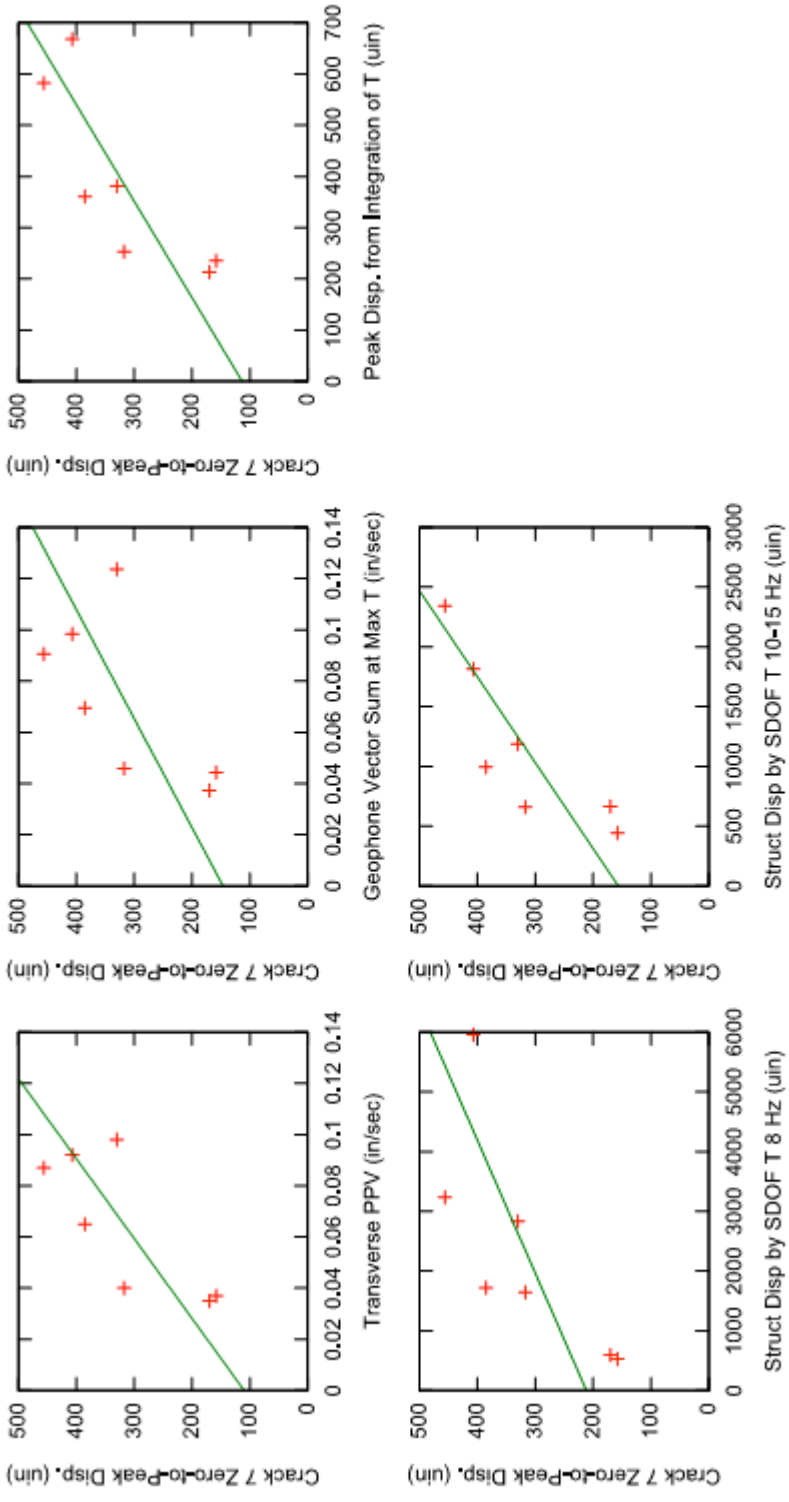

Figure 13: Selected sensitivity plots for Crack 7

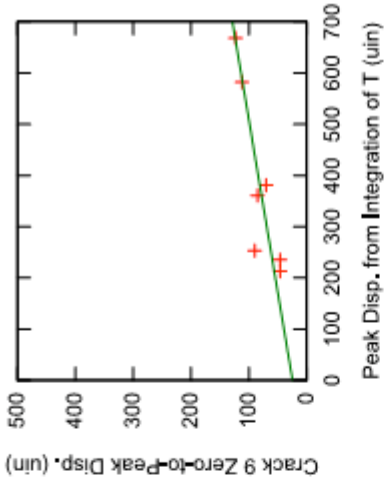

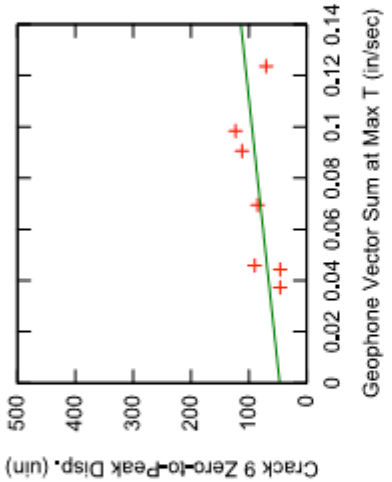

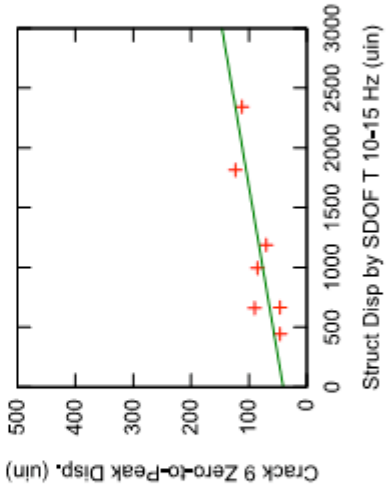

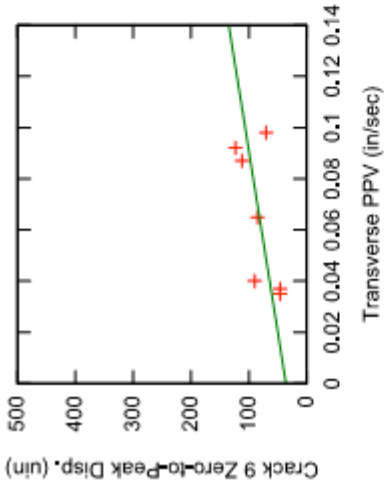

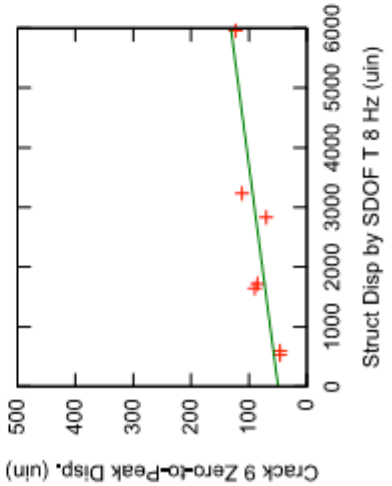

Figure 14: Selected sensitivity plots for Crack 9

Crack Response to Occupant Activity

Typical household activities, such as slamming doors and driving nails, were simulated on site to determine the magnitude and time history of the resulting vibration. All displacement and geophone channels were continuously recorded at 1000 samples per second. Table 2 summarizes these occupant activity tests. Figure 1 shows the response of Crack 7 to a person pounding on the wall near the crack with a fist.

Table 2: Summary of occupant activity tests

Test #	Description	Max zero-to-peak departure	
1	Pounding on door below Crack 7/Null 8	Crack 7	247 μin
2	Pounding on interior wall near Crack 7/Null 8	Crack 7	2523 μin
3	Closing overhead garage door (hard)	Geo T Crack 7	0.0263 in/sec 142 μin
4	Closing overhead garage door (softly)	no significant response on any channel	
5	Opening garage door	no significant response on any channel	
6	Pounding on exterior wall near Crack 9/Null 10	Crack 9	115 μin
7	Pounding on exterior wall near Crack 5/Null 6	Crack 5	53 μin

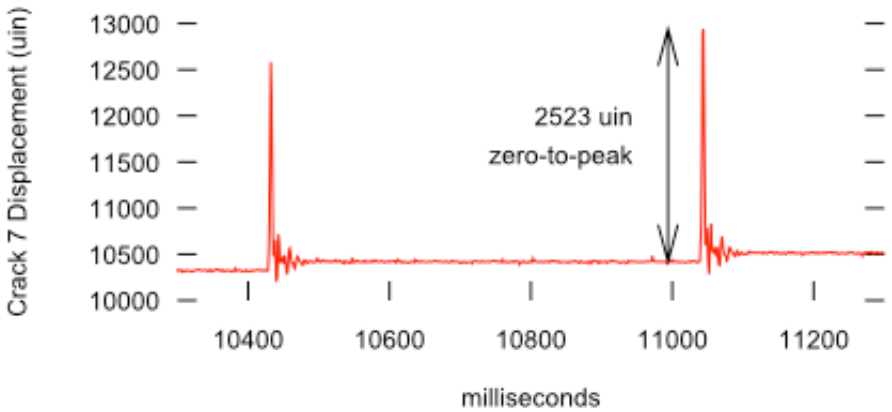

Figure 15: Crack 7 response to pounding on wall with fist

Crack Response to Environmental Effects

Residential structures, and thus their cracks, are typically sensitive to changes in temperature and relative humidity. These changes occur in daily, frontal, and seasonal patterns. On a typical July or August day, the outdoor gauge showed air temperature ranged from a low of 70° F to a high of 100° F, and outdoor relative humidity ranged from a low of 40% to a high of 95%. Recorded daily highs were greater than air temperatures because of the solar heating of the gauge on the south wall. Actual wall temperatures were likely to have been even greater. These daily cycles of expansion

and contraction, shown in red in Figures 16 and 17 silently induce strains in building materials.

Frontal and seasonal effects are also important. They can be identified through moving averages that smooth hourly crack displacement and environmental readings. A 24-hour central moving average was calculated at each hourly measurement, as described by McKenna (2002), and is shown in blue in Figures 16 and 17. The 24-hour central moving average for a given point is the mean of a total of 25 hourly measurements: twelve measurements before the given point, the point itself, and twelve measurements after the given point.

Previous studies, such as McKenna (2002) and Snider (2003), used the overall average over a monitoring period as a baseline for determining seasonal and extreme or unusual weather effects. Since the six-to-eight month span of this study is considerably longer than previous studies, the overall average approach would be misleading. Instead, a thirty-day central moving average was employed. The thirty-day central moving average is calculated in a manner similar to the 24-hour central moving average described above, and is shown in green in Figures 16 and 17.

Figures 16 and 17 compare the complete record of hourly crack displacement with the appropriate temperature and humidity readings. Graphical comparison of the 24-hour and thirty-day moving averages for temperature, humidity, and crack displacement clearly demonstrates that the three cracks are strongly influenced by weather changes. Figure 17 includes data from Null Sensor 8, which is located on an uncracked wall area near Crack 7. The data show that the sensor electronics are not subject to any significant drift due to changing environmental factors. This is consistent with previous studies involving eddy-current displacement sensors (Louis, 2000).

Daily, Frontal, and Weather Effects

Environmentally-driven crack responses fall into three categories: daily, frontal, and extreme/unusual weather effects, as shown in Figure 18. McKenna (2002) defined these in terms of hourly measurements, a 24-hour central moving average (CMA), and an overall average for the duration of monitoring. Since this report considers six months worth of data with apparent seasonal changes, a thirty-day central moving average is used in lieu of the overall average. The frontal effect is defined as the absolute value of the difference between peak 24-hour CMA values and the 30-day CMA. The daily effect is defined as the absolute value of the difference between the peak hourly measurements and the 24-hour CMA. Finally, the unusual/extreme weather effect is defined as the absolute value of the difference between peak hourly measurements and the 30-day CMA. Table 3 presents the maximum and average daily, frontal, and weather effects for the three cracks as well as temperature and humidity. Ratios of daily, climatological crack responses to blast induced crack responses are 27 and 100 for the exterior cracks and 16 for the interior garage crack

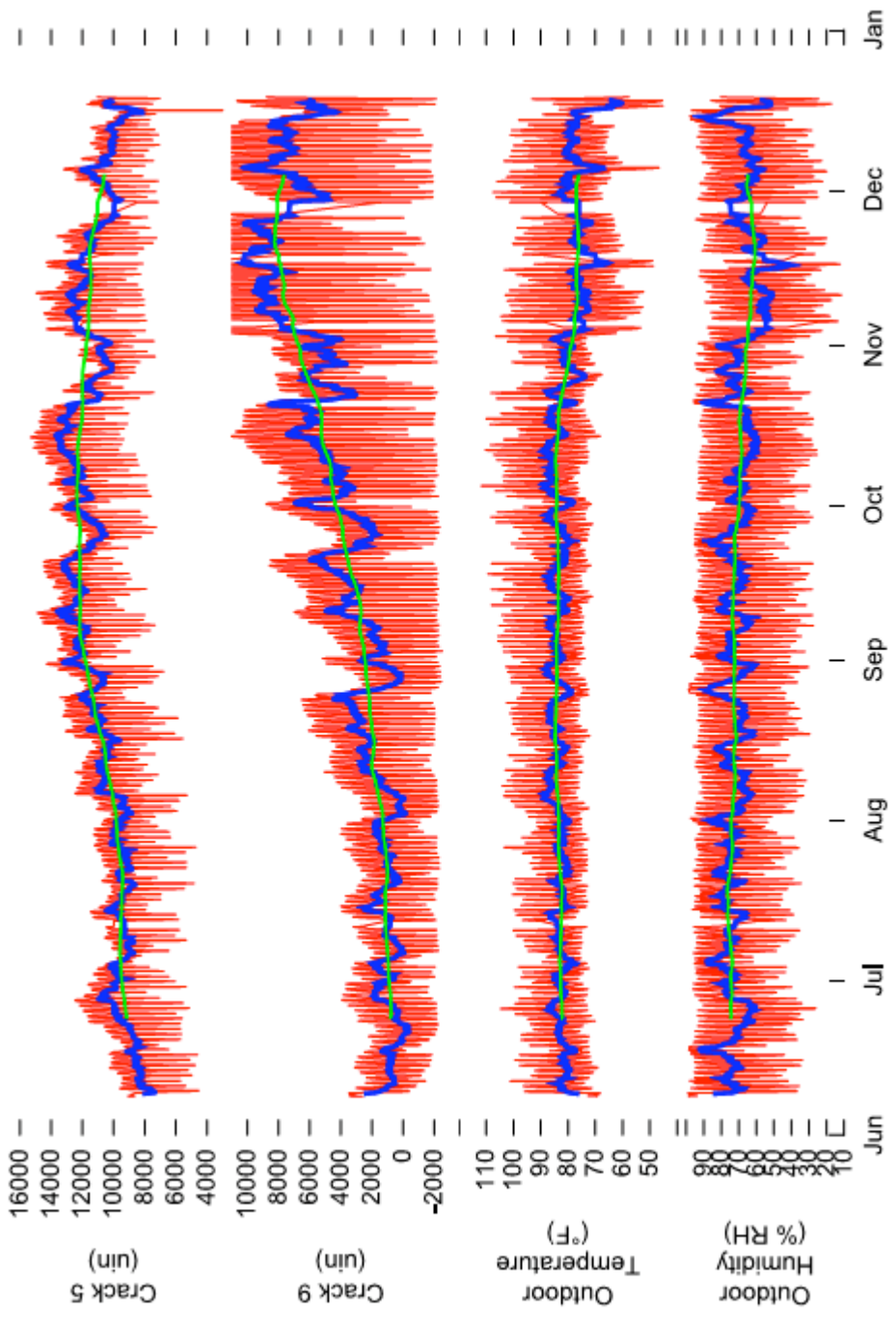

Figure 16: Comparison of hourly readings (shown in red) with 24-hour central moving average (blue) and 30-day central moving average (green) for exterior cracks and environmental conditions

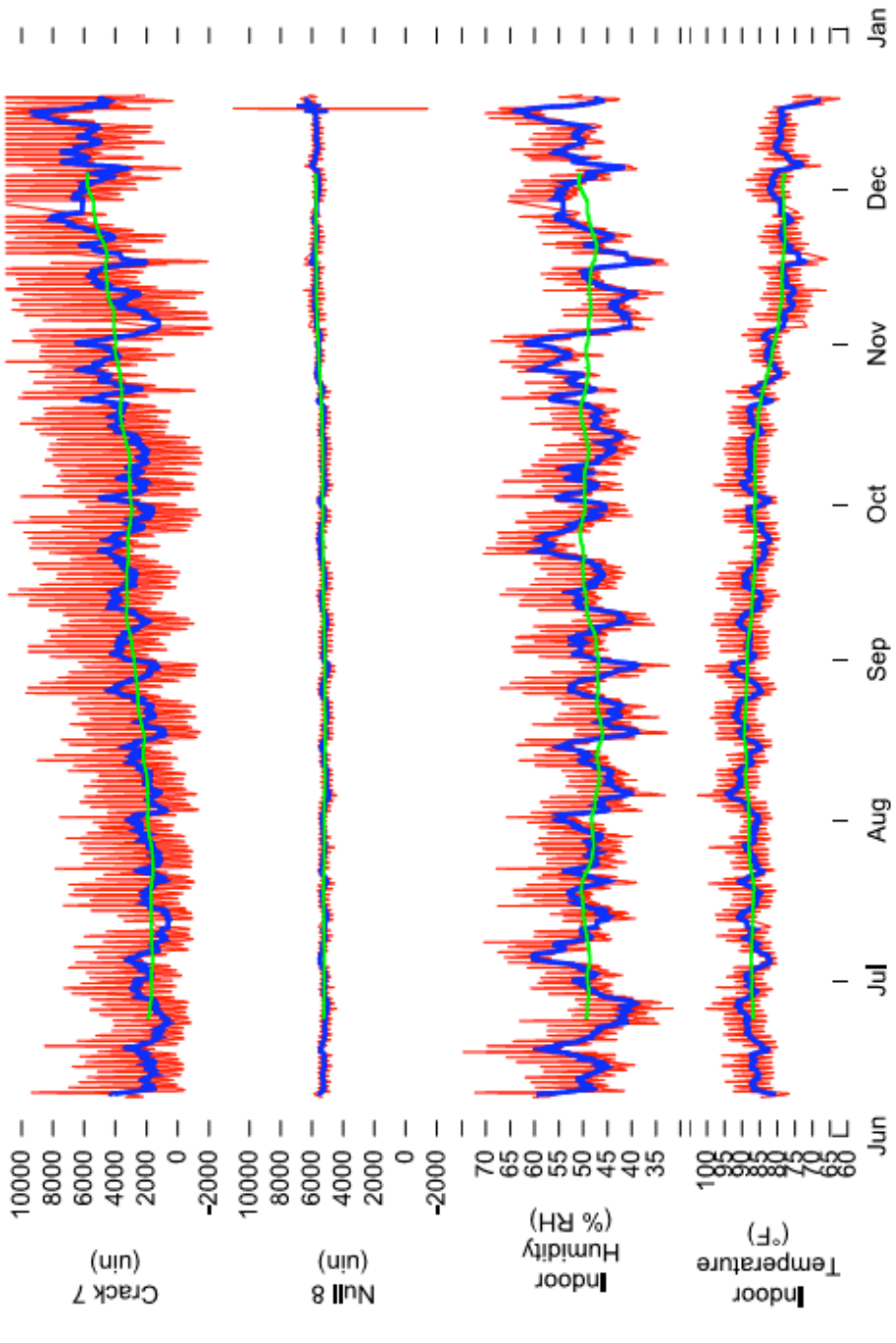

Figure 17: Comparison of hourly readings (shown in red) with 24-hour central moving average (blue) and 30-day central moving average (green) for interior crack, null sensor, and environmental conditions, showing sensitivity of crack to environmental conditions and negligible null sensor response

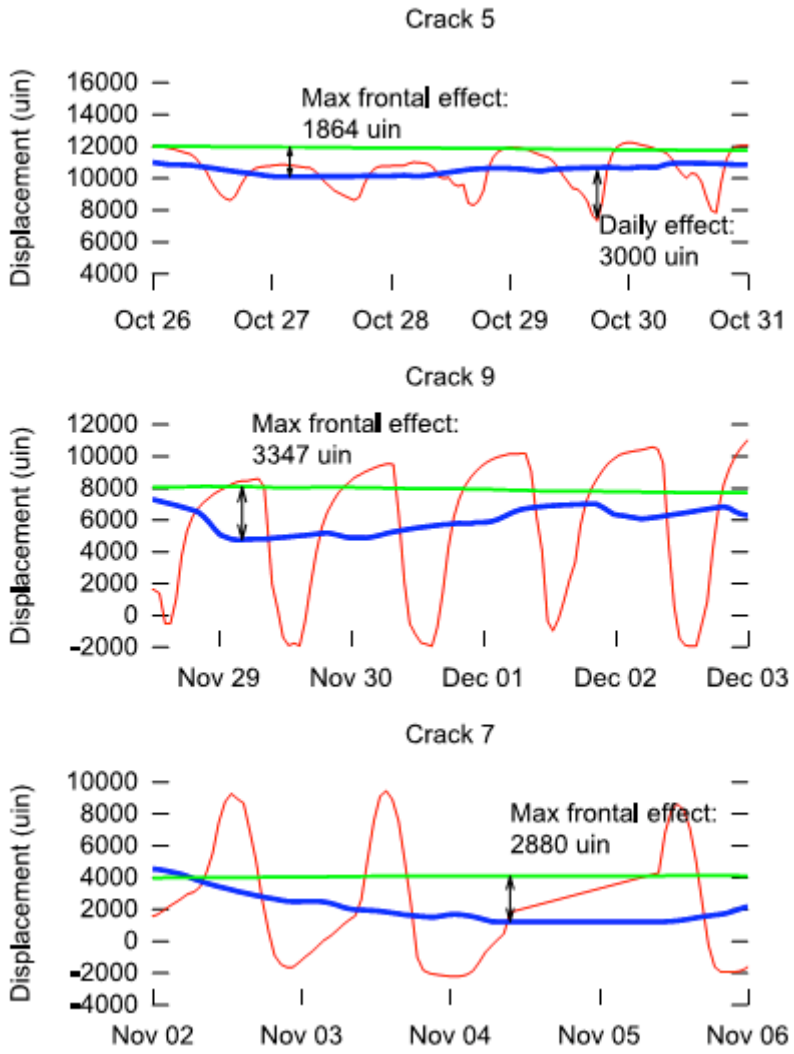

Figure 18: Expansion of five days in Figure 17 to illustrate how daily (red minus blue lines) and frontal (blue minus green lines) climatological effects are calculated from the 30 day (green) and 24 hour (blue) rolling average of the hourly readings (red)

Table 3: Zero-to-peak crack displacements due to daily, frontal, weather, and vibration effects

	Outdoor Temp. Change ° F	Outdoor Humidity Change % RH	Crack 5 Disp. μin	Crack 9 Disp. μin	-	Crack 7 Disp. μin	Indoor Temp. Change (° F)	Indoor Humidity Change % RH
Daily Effect								
Average	9	17	1263	2734		2168	3	4
Maximum overall	30	46	5410	10751		7872	11	18
Frontal Effect								
Average	2	5	564	902		714	2	4
Maximum overall	11	22	1864	3347		2880	6	13
Weather Effect								
Average	9	17	1343	2785		2212	3	5
Maximum overall	30	52	5256	9941		7798	14	21
Blast Effect								
Typical (Sept 7)	-	-	122	46		158	-	-
Maximum (Aug 15)	-	-	207	123		407	-	-

Long-Term (Climatological) vs. Vibration Effects

Silent climatological crack responses are larger than noisy vibratory/blast-induced crack responses. It is important to consider the relative magnitude of crack response induced by weather changes versus blasting. Figure 19 shows crack response from the August 21 blast in the context of daily changes in temperature and humidity. This blast produced the largest crack response and ground motions within 8% of the largest ground motions recorded in this study. In each case, the climatological change in response on the day of the blast is an order of magnitude greater than the dynamic response during the blast. This difference is even greater for blasts that produced small ground motions.

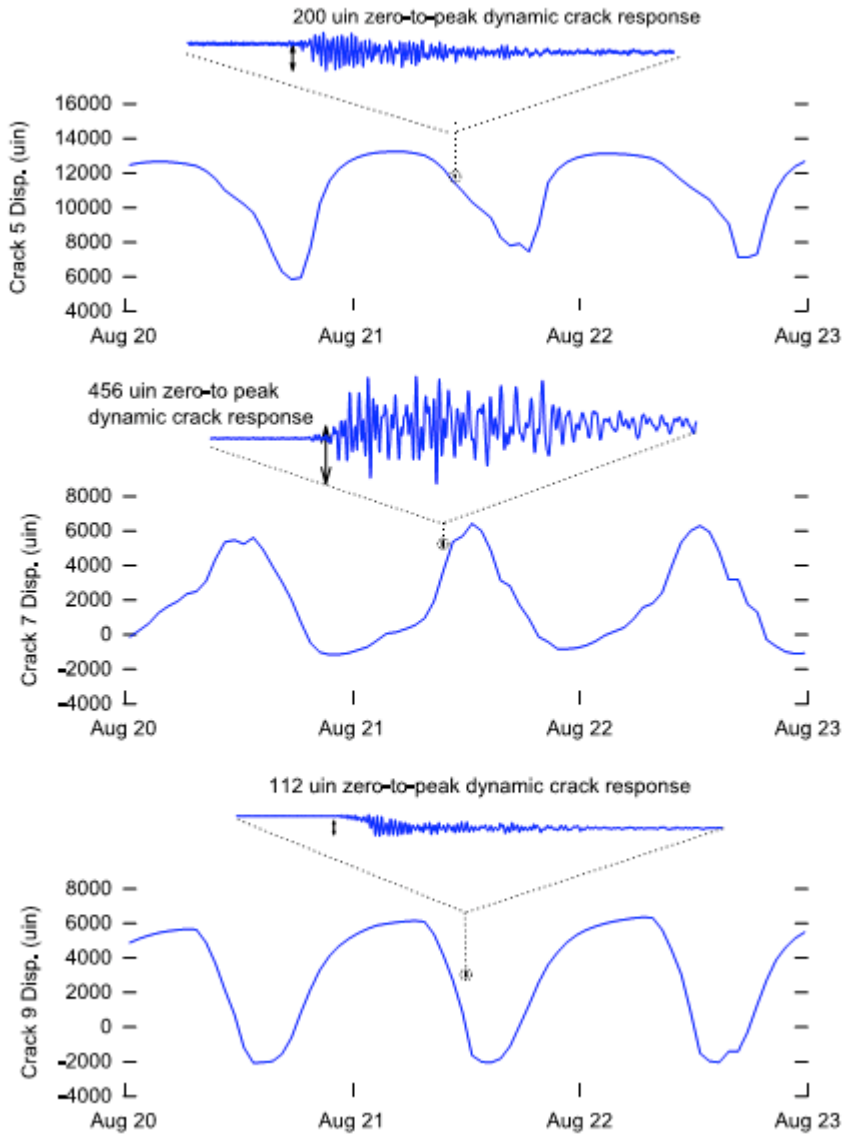

Figure 19: The dot inside the small, dotted black circle provides a visual comparison with the large, long term climatologically induced crack responses (solid, slowly varying line) and the vibratory crack responses (dot). Vibration response inside the dot is enlarged via the sloping dotted line and placed above the climatological response. Presentation technique after Aimone-Martin and Rosenhaim (2007).

Comparison of Crack Response to Ground Motion, Occupant Activity, and Environmental Effects

Figure 20 compares the response of the three cracks to daily, frontal, and maximum weather effects with dynamic responses produced by occupant activities and blast-induced ground motion. The August 21 blast is featured for blast effects because the largest crack response recorded during the study (456μin on Crack 7) occurred during that event. The September 7 blast (with a peak particle velocity of 0.037 ips) is a more typical event.

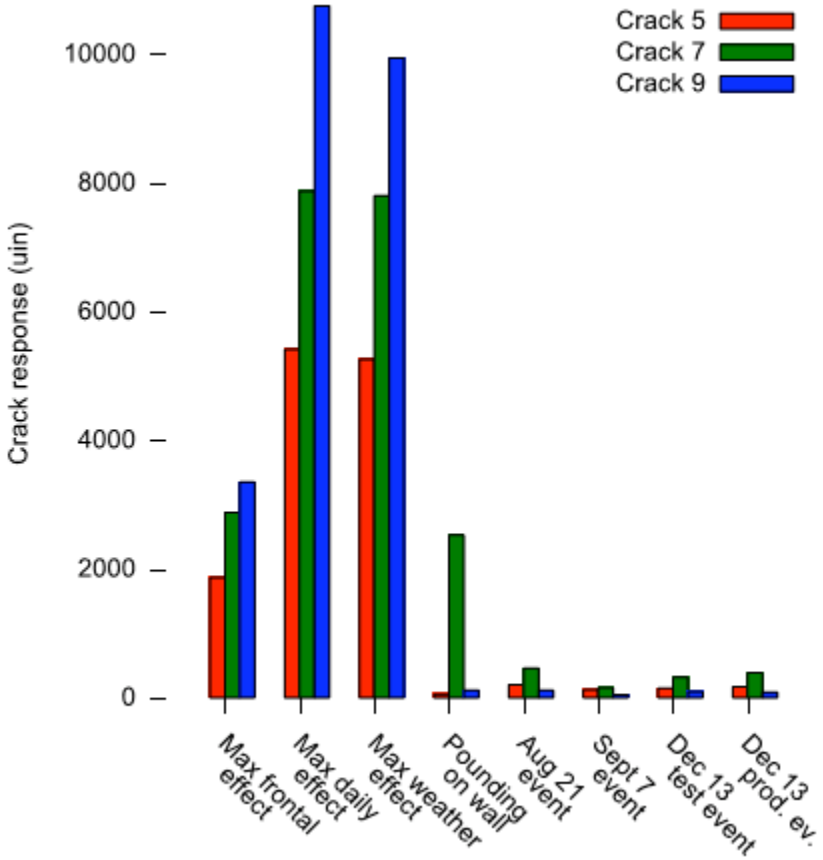

Figure 20: Comparison of crack response to environmental effects, occupant activity, and blast-induced ground motion. Peak particle velocity in the plane of the cracks for August 21, September 7, December 13 test, and December 13 production event is 0.087, 0.037, 0.040, and 0.065 in/sec, respectively.

Communication

Responses must be transmitted from the test house to the central digital repository for processing in a timely manner in order to be useful. Since recording of dynamic events creates a large volume of data, it is preferable to transmit the data via a high-speed Internet connection. It is important to minimize the communication time

because the data acquisition system is not able to record new data while old data is being uploaded. Unfortunately, no practical high-speed Internet connection was available at the residence. However, such a connection was available at the on-site trailer at the quarry, 1.6 miles away. Consequently, the communication link between the laboratory and the data acquisition system in the field consists of first connecting the residence to the quarry trailer and then connecting the trailer to the laboratory.

The Northwestern system communicated between the residence and the quarry trailer via a FreeWave HTPlus industrial wireless Ethernet link. High-gain Yagi antennas aligned via compass bearings were installed to maximize communication reliability through the 1.6 miles of dense vegetation between the residence and the trailer. Data transmission rates of 154 kb/sec are regularly realized.

The trailer end of the wireless Ethernet link is connected to an existing consumer-grade DSL modem and router in the trailer. This DSL connection provided a convenient Internet connection point. An industrial hardware VPN unit was deployed at the residence in order to reliably traverse the router's network address translation system.

Autonomous Operation

Perhaps the most important aspect of this continuous remote monitoring installation is its autonomous operation. Data from the Northwestern instruments are continuously acquired by the on-site datalogger at all times except during a nightly download window of less than 15 minutes. Every night, data are downloaded from the remote field computer, converted from the field computer's proprietary data format, archived in the project database, and displayed on the project Web site without any human intervention. Figure 21 shows the autonomous data flow from field site to end users.

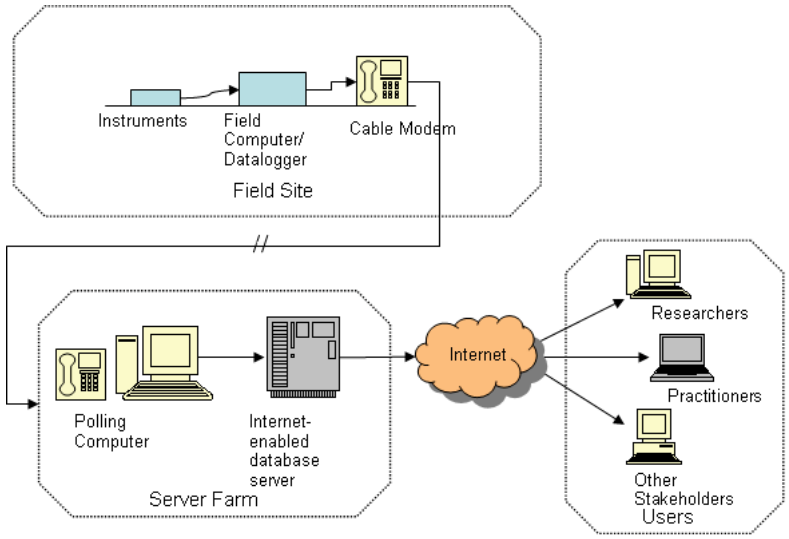

Figure 21: Flow of remote monitoring data from field instruments to central digital repository and Web site (Kosnik, 2007)

Project Web Sites

Data recorded by both the Northwestern and GeoSonics systems at the house are presented on Web sites for review and analysis. Since measurements from field sites are much more readily useful if they become available in a timely manner, custom software was developed to archive and display data in an Internet-accessible relational database as they arrive (Kosnik, 2007). This Internet-enabled data management system eliminates barriers that often prevent the full and timely utilization of remotely acquired data, including such tasks as manually downloaded, parsing, and plotting new data. Storing all project data in an Internet-accessible relational database also eliminates the need to traverse multiple data files in order to find data of interest. The long-term and dynamic event data from the Northwestern crack monitoring system are displayed automatically on a site hosted by Civil Data Systems for the Northwestern University Infrastructure Technology Institute (ITI)[1]. The GeoSonics data are presented on two distinct Web sites. The GeoSonics-Civil Data Systems site[2] is automatically updated in the same way as the Northwestern site. The other site[3] is hosted by GeoSonics and is manually updated with shot summaries only.

Both the Northwestern and GeoSonics-Civil Data Systems sites are password-protected so authorized parties may view the data. With this password system, the site can be opened to quarry neighbors in the future. In this capacity, the Web site would act as a powerful communication tool. It will be possible to display data within 24 hours of an event, as data are transmitted to the host computer in the early morning. Records will be checked to ensure that actual quarry blasts are reported. For example, it is important to distinguish occupant- or weather-induced response (e.g., thunderstorms) from true blast-induced responses. Figure 22 is an example web page from the Northwestern instrumentation Web site.

[1] http://iti.jones.civildata.com/
[2] http://jones.civildata.com/
[3] http://www.jonesmining.info/

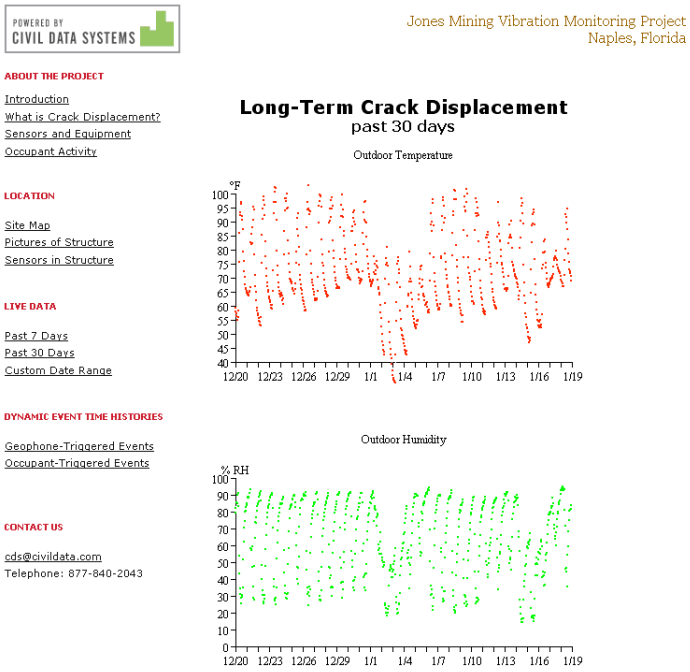

Figure 22: Screen capture of remote monitoring Web site, showing automatically-generated plots of near-real time data from the test house

CONCLUSIONS

This report has described the autonomous remote measurement of microinch responses of cosmetic cracks in a residence near a limestone quarry. Microinch-resolution displacement transducers were used to measure the change in crack width in response to vibration from blasting, occupant activity, and changes in temperature and humidity. For each of the three instrumented cracks, the response to daily, frontal, and seasonal changes in temperature and humidity was more than ten times greater than the response to blast vibration. Quantitative, scientific measurements of these phenomena contrast sharply with the qualitative perception, based on human senses, that blast vibrations are disruptive.

Commercial off-the-shelf sensors and a general-purpose commercial data acquisition system were used in conjunction with specialized communication equipment and custom software to create a robust autonomous method to record sensor signals, transmit them to a central repository, and distribute them in a readily useful format via the Internet for interpretation, without human intervention.

References

Aimone-Martin, C. and Rosenhaim, V. (2007). Structure response study at the Pineville Quarry. Technical report, Aimone-Martin Associates LLC, Socorro, New Mexico.

Baillot, R. (2004). Crack response of a historic structure to weather effects and construction vibrations. Master's thesis, Northwestern University, Evanston, Illinois.

Chok, K. (2003). NUVIB 2: Northwestern University Vibration Analysis 2. Computer program.

Dowding, C. and Aimone-Martin, C. (2007). Micro-meter crack response to rock blast vibrations, wind gusts, and weather effects. In *Proc. Geo-Denver 2007*, Denver, Colorado. American Society of Civil Engineers.

Dowding, C. H. (1996). *Construction Vibrations*. Prentice Hall, Upper Saddle River, New Jersey.

Dowding, C. H. and McKenna, L. M. (2005). Crack response to long-term environmental and blast vibration effects. *Journal of Geotechnical and Geoenvironmental Engineering*, 131(9).

Jones, D. (2007). Personal communication.

Kosnik, D. E. (2007). Internet-enabled geotechnical data exchange. In *Proc. 7th Int'l Symposium on Field Measurements in Geomechanics*, Boston, Massachusetts. American Society of Civil Engineers.

Louis, M. (2000). Autonomous Crack Comparometer Phase II. Master's thesis, Northwestern University, Evanston, Illinois.

McKenna, L. M. (2002). Comparison of measured crack response in diverse structures to dynamic events and weather phenomena. Master's thesis, Northwestern University, Evanston, Illinois.

Siebert, D. (2000). Autonomous Crack Comparometer. Master's thesis, Northwestern University, Evanston, Illinois.

Snider, M. (2003). Crack response to weather effects, blasting, and construction vibrations. Master's thesis, Northwestern University, Evanston, Illinois.